Disorder-induced phonon self-energy of semiconductors with binary isotopic composition

F. Widulle, J. Serrano, and M. Cardona
Max-Planck-Institut für Festkörperforschung, Heisenbergstrasse 1, D-70569 Stuttgart, Germany
(Received 29 May 2001; published 18 January 2002)

Self-energy effects of Raman phonons in isotopically disordered semiconductors are deduced by perturbation theory and compared to experimental data. In contrast to the acoustic frequency region, higher-order terms contribute significantly to the self-energy at optical phonon frequencies. The asymmetric dependence of the self-energy of a binary isotope system $m_{1-x}M_x$ on the concentration of the heavier isotope mass x can be explained by taking into account second- and third-order perturbation terms. For elemental semiconductors, the maximum of the self-energy occurs at concentrations with $0.5<x<0.7$, depending on the strength of the third-order term. Reasonable approximations are imposed that allow us to derive explicit expressions for the ratio of successive perturbation terms of the real and the imaginary part of the self-energy. This basic theoretical approach is compatible with Raman spectroscopic results on diamond and silicon, with calculations based on the coherent potential approximation, and with theoretical results obtained using *ab initio* electronic theory. The extension of the formalism to binary compounds, by taking into account the eigenvectors at the individual sublattices, is straightforward. In this manner, we interpret recent experimental results on the disorder-induced broadening of the TO (folded) modes of SiC with a ^{13}C-enriched carbon sublattice [S. Rohmfeld, M. Hundhausen, L. Ley, N. Schulze, and G. Pensl, Mater. Sci. Forum **338-342**, 579 (2000); Phys. Rev. Lett. **86**, 826 (2001)].

DOI: 10.1103/PhysRevB.65.075206 PACS number(s): 78.30.Ly, 63.20.−e, 63.50.+x

I. INTRODUCTION

The mass fluctations (of a single element) induced by isotopic disorder can be described by the weighted nth moments of the relative mass differences with respect to the average mass $\overline{m}$ of the virtual crystal, defined as

$$g_n=\sum_i c_i\left(\frac{\overline{m}-m_i}{\overline{m}}\right)^n, \tag{1}$$

where i runs over the different isotopes with masses m_i and concentrations c_i. The definition of the average mass $\overline{m}=\Sigma_i c_i m_i$ implies that $g_1=0$.

For a two-isotope system $m_{1-x}M_x$ with M being the heavy mass and $x=c_M$, Eq. (1) reads

$$g_n(x)=(1-x)\left(\frac{\overline{m}-m}{\overline{m}}\right)^n+x\left(\frac{\overline{m}-M}{\overline{m}}\right)^n. \tag{2}$$

Equation (2) can be rewritten as follows, using $\Delta m=M-m$

$$g_n(x)=(m/\Delta m+x)^{-n}x(1-x)\times[x^{n-1}+(-1)^n(1-x)^{n-1}]. \tag{3}$$

For the elements under consideration here [$\Delta m/m\ll 1$, e.g. $(\Delta m/m)_C=1/12$] we can neglect the x dependence of the first factor of Eq. (3), which slightly breaks the odd or even symmetry of $g_n(x)$ with respect to $x=0.5$. Thus, for $x\ll m/\Delta m$ with $0\leqslant x\leqslant 1$ we can write

$$(m/\Delta m+x)^{-n}\simeq(\Delta m/m)^n. \tag{4}$$

The lowest-order moments of g_n thus read (see Fig. 1):

$$g_2\simeq(\Delta m/m)^2x(1-x), \tag{5a}$$

$$g_3\simeq(\Delta m/m)^3x(1-x)(2x-1), \tag{5b}$$

$$g_4\simeq(\Delta m/m)^4x(1-x)[1-3x(1-x)], \tag{5c}$$

$$g_5\simeq(\Delta m/m)^5x(1-x)(2x-1)[1-2x(1-x)]. \tag{5d}$$

Hence, the contribution to the self-energy is even (odd) with respect to $x=0.5$ for even (odd) values of n. In particular, g_2 represents a parabola with the maximum at $x=0.5$, while g_3 is odd with respect to $x=0.5$, i.e., $g_3(0.5)=0$.

The disorder-induced phonon self-energy is defined as

$$\Pi_{\rm dis}(\omega)=\Delta_{\rm dis}(\omega)-i\Gamma_{\rm dis}(\omega)/2, \tag{6}$$

where $\Delta_{\rm dis}$ denotes the disorder-induced shift, and $\Gamma_{\rm dis}$ the disorder-induced broadening corresponding to the full width at half maximum (FWHM). The self-energy can be decomposed into individual contributions that are proportional to the various moments of g_n with $n=2,3,4,\ldots,$

$$\Pi_{\rm dis}(\omega)=A_2x(1-x)+A_3x(1-x)(2x-1)+A_4x(1-x)[1-3x(1-x)]+\cdots. \tag{7}$$

In order to estimate the contributions of higher-order perturbation terms, Eq. (7) is fitted to experimental and theoretical data of group-IV semiconductors (see Sec. III for diamond, Si, Ge, α-Sn and Sec. IV for SiC). In Eq. (7) the fit parameters $A_i=A_{i,\Delta}+iA_{i,\Gamma}$ are complex numbers; in prac-

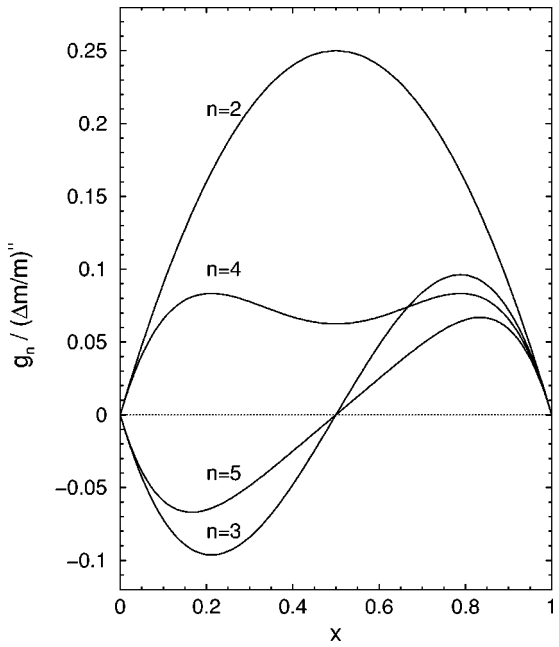

FIG. 1. Mass fluctuations $g_n(x)$ for various nth moments [Eq. (5)] of an elemental, i.e., monoatomic, crystal (or each sublattice of a compound) containing a binary isotope system. x denotes the concentration of the heavier mass isotope.

tice, we perform individual fits to $\Delta_{\rm dis}$ and $\Gamma_{\rm dis}$, thus obtaining the two sets of fit parameters $A_{i,\Delta}$ and $A_{i,\Gamma}$. In the following section we show that, in general, the asymmetries with respect to $x=0.5$ are not identical for $\Delta_{\rm dis}$ and $\Gamma_{\rm dis}$.

For a characterization of the contribution of the third-order perturbation term with respect to the second-order term, we define the ratio

$$r_s=\frac{A_{3,s}}{A_{2,s}} \tag{8}$$

with $s=\Delta,\Gamma$. For the maximum self-energy $x_{\max,s}$ we find

$$x_{\max,s}=\frac{1}{2}\pm\frac{1}{6}\left(\sqrt{3+\frac{1}{r_s^2}}-\frac{1}{|r_s|}\right), \tag{9}$$

where the positive (negative) sign corresponds to $r>0$ $(r<0)$.

II. PERTURBATION THEORY

In this section, explicit expressions for the disorder-induced self-energies of a two-isotope elemental crystal are derived by perturbation theory. For the calculations we use $\Pi_{\rm dis}=\Pi=\Delta+i\Gamma$ with $\Delta=\Delta_2+\Delta_3+\cdots=\Delta_{\rm dis}$ and $\Gamma=\Gamma_2+\Gamma_3+\cdots=-\Gamma_{\rm dis}/2$. The zero-temperature phonon propagator[1] $D(\omega,\omega_i)$ for an isotopically pure crystal is the sum of the propagators $D_+(\omega,\omega_i)$ and $D_-(\omega,\omega_i)$ for positive and negative frequencies, respectively,

$$D=D_+(\omega,\omega_i)+D_-(\omega,\omega_i) \tag{10a}$$

$$=\frac{1}{\omega-\omega_i-i\gamma}+\frac{1}{-\omega-\omega_i-i\gamma} \tag{10b}$$

$$=\frac{2\omega_i}{\omega^2-\omega_i^2-i2\omega_i\gamma}, \tag{10c}$$

where $\gamma\to 0$ if anharmonicity is neglected. ω_i denotes the absolute value of the phonon frequency. Since we are interested in the self-energy of the Raman mode, to which the largest contributions stem from close-lying optic phonon states, the propagator D_- can be neglected because $|{\rm Re}\{D_-\}|\ll|{\rm Re}\{D_+\}|$ and $|{\rm Im}\{D_-\}|\ll|{\rm Im}\{D_+\}|$. In the following we thus set $D=D_+$ with

$$D_+(\omega,\omega_i)=\frac{1}{\omega-\omega_i-i\gamma} \tag{11a}$$

$$=\frac{\omega-\omega_i}{(\omega-\omega_i)^2+\gamma^2}+i\frac{\gamma}{(\omega-\omega_i)^2+\gamma^2} \tag{11b}$$

$$=P_i(\omega)+iL_i(\omega). \tag{11c}$$

$D_+(\omega,\omega_i)$ consists of $P_i(\omega)$, with a pole at ω_i, and a Lorentzian $L_i(\omega)$. For the complex self-energy of the Raman phonon of a semiconductor with diamond structure, nth-order perturbation theory yields[2]

$$\Pi_n(\omega,x)=\frac{g_n(x)}{2^n}\omega\left(\frac{1}{6N_c}\right)^{n-1}$$

$$\times\sum_{i_1,i_2,\ldots,i_{n-1}}\omega_{i_1}D_{i_1}\cdot\omega_{i_2}D_{i_2}\cdots\omega_{i_{n-1}}D_{i_{n-1}} \tag{12a}$$

$$=\frac{g_n(x)}{2^n}\omega\left(\frac{1}{6N_c}\sum_i\omega_iD_i\right)^{n-1} \tag{12b}$$

with $D_i=D(\omega,\omega_i)$ and N_c the number of unit cells. Note that a factor of $(-1)^n$ is found in the corresponding equation of the self-energy in Ref. 2. We believe that this factor should not be there when the definition of g_n given in Ref. 2 [the same as our Eq. (1)] is used. The factor appears only if $m_i-\overline{m}$ is written instead of $\overline{m}-m_i$ inside the brackets of Eq. (1). It is easy to convince oneself of this fact by comparing the real part of the third-order self-energy with the standard expression from static perturbation theory which can be found in Ref. 3.

The second-order term $(n=2)$ of the self-energy

$$\Pi_2(\omega,x)=\frac{g_2(x)}{4}\omega\left(\frac{1}{6N_c}\sum_i\omega_i(P_i+iL_i)\right) \tag{13a}$$

contains the real part

$$\Delta_2(\omega,x)=\frac{g_2(x)}{4}\omega\left(\frac{1}{6N_c}\sum_i\ \omega_i\frac{\omega-\omega_i}{(\omega-\omega_i)^2+\gamma^2}\right) \tag{13b}$$

and the imaginary part

$$\Gamma_2(\omega,x)=\frac{g_2(x)}{4}\omega\left(\frac{1}{6N_c}\sum_i\ \omega_i\frac{\gamma}{(\omega-\omega_i)^2+\gamma^2}\right). \tag{13c}$$

For $\gamma\to 0$, Eq. (13c) simplifies to a sum over δ-functions, which represents the one-phonon density of states (DOS) $\rho_1(\omega)$,

$$-\Gamma_2(\omega,x)=\frac{g_2(x)}{4}\omega^2\left(\frac{1}{6N_c}\sum_i\ \pi\delta(\omega-\omega_i)\right) \tag{13d}$$

$$=\frac{\pi}{24}g_2(x)\omega^2\rho_1(\omega). \tag{13e}$$

If $\Delta_2(\omega)$ and $\Gamma_2(\omega)$ do not depend strongly on ω near the Raman phonon at ω_0, then $-\Gamma_2(\omega_0)$ of Eq. (13e) represents the half width at half maximum (HWHM) of the disorder-induced broadening.

The third-order self-energy can be written as

$$\Pi_3(\omega,x)=\frac{g_3(x)}{8}\omega\left(\frac{1}{6N_c}\right)^2\sum_{i,j}\ \omega_i\omega_j(P_i+iL_i)(P_j+iL_j), \tag{14a}$$

yielding the following real and imaginary parts:

$$\Delta_3(\omega,x)=\frac{g_3(x)}{8}\omega\left(\frac{1}{6N_c}\right)^2\sum_{i,j}\ \omega_i\omega_j(P_iP_j-L_iL_j), \tag{14b}$$

$$\Gamma_3(\omega,x)=\frac{g_3(x)}{4}\omega\left(\frac{1}{6N_c}\right)^2\sum_{i,j}\ \omega_i\omega_jP_iL_j. \tag{14c}$$

The corresponding fourth-order terms read

$$\Delta_4(\omega,x)=\frac{g_4(x)}{16}\omega\left(\frac{1}{6N_c}\right)^3\times\sum_{i,j,k}\ \omega_i\omega_j\omega_k(P_iP_jP_k-3L_iL_jP_k), \tag{15a}$$

$$\Gamma_4(\omega,x)=\frac{g_4(x)}{16}\omega\left(\frac{1}{6N_c}\right)^3\times\sum_{i,j,k}\ \omega_i\omega_j\omega_k(3P_iP_jL_k-L_iL_jL_k). \tag{15b}$$

The ratios of the third-order to the second-order perturbation terms for the real and imaginary part of the self-energy is simply related to the disorder-induced shift Δ_2 and broadening Γ_2:

$$\frac{\Delta_3}{\Delta_2}=\frac{g_3(x)}{2g_2(x)}\frac{1}{6N_c}\frac{\left(\sum_i\ \omega_iP_i\right)^2-\left(\sum_i\ \omega_iL_i\right)^2}{\sum_i\ \omega_iP_i}$$

$$=2\frac{g_3(x)}{g_2(x)}\frac{1}{\omega}\left[\frac{\Delta_2^2-\Gamma_2^2}{g_2\Delta_2}\right]_{x=x_0}, \tag{16a}$$

$$\frac{\Gamma_3}{\Gamma_2}=\frac{g_3(x)}{g_2(x)}\frac{1}{6N_c}\sum_i\ \omega_iP_i$$

$$=4\frac{g_3(x)}{g_2(x)}\frac{1}{\omega}\left[\frac{\Delta_2}{g_2}\right]_{x=x_0}. \tag{16b}$$

The ratios r_s [Eq. (8)] for a certain phonon mode at ω_0 can be determined from the dilute limits $x\to\{0,1\}$ and the experimental shifts and broadenings for $x_0=0.5$. Under the approximation of Eq. (4), the expressions of Eqs. (16a) and (16b) simplify to

$$r_\Delta\simeq 8\frac{m}{\Delta m}\frac{1}{\omega}\left[\frac{\Delta_2^2-\Gamma_2^2}{\Delta_2}\right]_{x_0=0.5}, \tag{17a}$$

$$r_\Gamma\simeq 16\frac{m}{\Delta m}\frac{1}{\omega}[\Delta_2]_{x_0=0.5}. \tag{17b}$$

For phonons of crystals whose $|\Delta_2(\omega_0,x_0)|$ and $|\Gamma_2(\omega_0,x_0)|$ are comparable, such as for the Raman mode of diamond or the TO Raman modes of SiC, the asymmetry of $\Delta(\omega_0,x)$ also depends on $\Gamma_2(\omega_0,x_0)$ and $r_\Gamma/r_\Delta\propto 2\Delta_2^2/(\Delta_2^2-\Gamma_2^2)$ ($r_\Gamma/r_\Delta\approx 8/3$ for the Raman mode of diamond).

For phonons with $|\Gamma_2(\omega_0)|\ll|\Delta_2(\omega_0)|$, such as the Raman modes of Si, Ge, and α-Sn, Eq. (17a) can be further simplified. In these cases, $r_\Delta\propto\Delta_2$ and $r_\Gamma/r_\Delta\simeq 2$. The fact that, generally, the contributions of higher-order terms to the self-energy are not equally distributed among the real and the imaginary part ($r_\Delta\neq r_\Gamma$) means, that the asymmetries of $\Delta(\omega_0,x)$ and $\Gamma(\omega_0,x)$ have different shapes resulting in different concentrations at the maximum self-energies ($x_{\max,\Delta}\neq x_{\max,\Gamma}$). The ratios of the next successive-order terms read

$$\frac{A_{4,\Gamma}}{A_{3,\Gamma}}=\frac{3}{4}\frac{A_{3,\Gamma}}{A_{2,\Gamma}}=\frac{3}{2}\frac{A_{4,\Delta}}{A_{3,\Delta}}=\frac{3}{2}\frac{A_{3,\Delta}}{A_{2,\Delta}}. \tag{18}$$

Figure 2 shows the dependence on r_s of the concentration $x_{\max}$, at which the self-energy has a maximum, if $|\Gamma_2(\omega_0)|\ll|\Delta_2(\omega_0)|$ (valid for Si, Ge, and α-Sn).

General expressions for the ratios of successive-order perturbation terms for phonons with $|\Gamma_2(\omega_0)|\ll|\Delta_2(\omega_0)|$ can be easily found using

$$\left(\sum_i\ \omega_iD_i\right)^n=\left(\sum_i\ \omega_iP_i+i\sum_i\ \omega_iL_i\right)^n=\eta^ne^{in\theta}$$

$$=\eta^n[\cos(n\theta)+i\sin(n\theta)]\simeq\eta^n(1+in\theta), \tag{19}$$

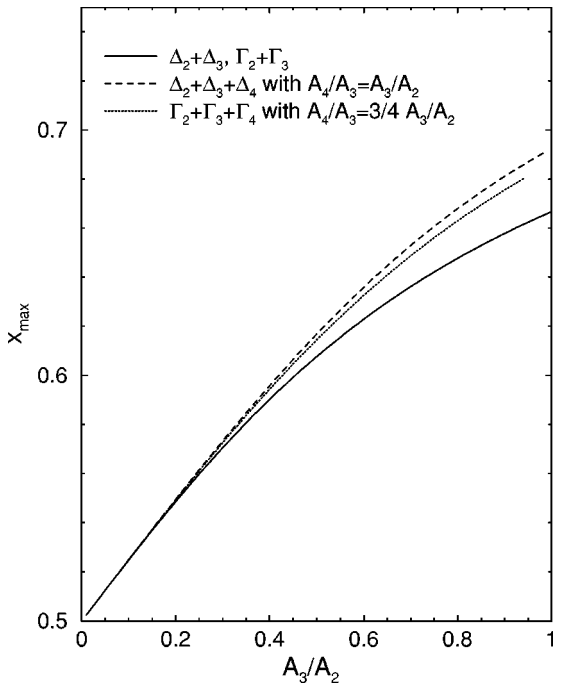

FIG. 2. Dependence of the value of $x_{\max}$ at which the maximum of Δ and Γ is found, including second-order and third-order perturbation terms (solid line) and also fourth-order terms (dashed and dotted lines).

where $\eta=|\Sigma_i \omega_i D_i|$ and $\theta=\mathrm{Arg}\{\Sigma_i \omega_i D_i\}$. They are

$$\frac{\Delta_{n+1}}{\Delta_n}=\frac{g_{n+1}}{2g_n}\left(\frac{1}{6N_c}\sum_i \omega_i P_i\right) \tag{20a}$$

$$\frac{\Gamma_{n+1}}{\Gamma_n}=\frac{g_{n+1}}{2g_n}\frac{n}{n-1}\left(\frac{1}{6N_c}\sum_i \omega_i P_i\right) \tag{20b}$$

$$=\frac{n}{n-1}\frac{\Delta_{n+1}}{\Delta_n}. \tag{20c}$$

According to Eq. (17a), negative values for r_Δ are possible if $|\Gamma_2|$ exceeds $|\Delta_2|$, but this does not occur for the Raman phonons of elemental semiconductors. One could also obtain $r_\Gamma<0$ [Eq. (17b)] for phonons with $\mathbf{q}\neq 0$ that exhibit a negative disorder-induced shift.[4] The latter originates from the fact that the shift is related to the Kramers-Kronig transformation of the broadening, which displays a change of sign of $\Delta_{\mathrm{dis}}(\omega)$ near maxima of $\Gamma_{\mathrm{dis}}(\omega)$. In such a case the asymmetry would be flipped with respect to $x=0.5$, i.e., the maximum of the self-energy would occur at a concentration $x_{\max}<0.5$.

III. COMPARISON WITH EXPERIMENTAL AND THEORETICAL RESULTS

In this section, we display a compilation of the disorder-induced self-energies for the Raman phonons of elemental crystals (diamond, Si, Ge, α-Sn) which have been obtained either by Raman spectroscopy or from theoretical calculations by several research groups during the past decade. Raman studies that address the variation of the self-energy with the isotopic composition have been conducted for diamond[5–10] and Si.[11] The coherent potential approximation (CPA) has been employed for diamond[6–8] and Si,[11] while *ab initio* electronic structure based calculations have been performed for diamond and Ge.[12,13] All sets of data are analyzed with respect to the asymmetries of the self-energies and compared to the results we obtain by perturbation theory.

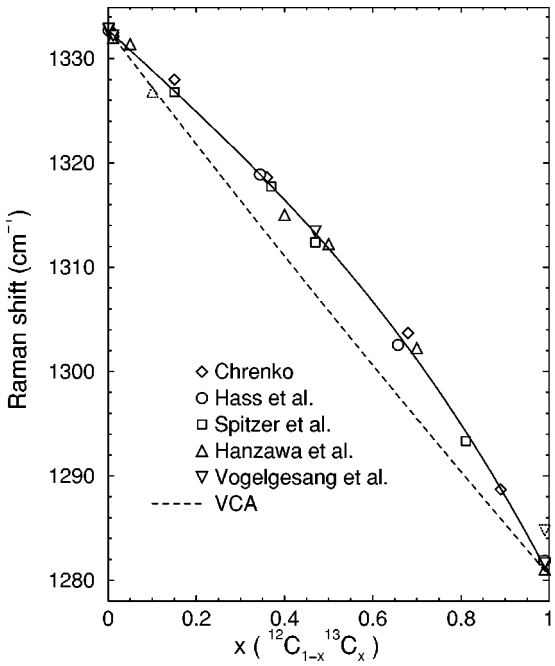

FIG. 3. Raman shift of isotopically disordered diamond. The open symbols represent experimental values (Refs. 5–10). The dashed line indicates the harmonic scaling of the phonon frequency within the VCA ($\omega\propto\bar{m}^{-1/2}$). The solid line corresponds to a fit with Eq. (7) for $n=2,3$ to all experimental data, added to the VCA scaling. The two experimental data points at $x=0.1$ and $x=1$, represented as dotted symbols, were excluded from this fit.

Figure 3 displays the Raman frequencies of diamond versus the ^{13}C concentration. The points (open symbols) represent experimental values. The dashed curve represents the approximately linear dependence expected in the VCA. The upward curvature of the experimental data (with respect to the VCA line) clearly demonstrates the existence of an isotopic-disorder-induced self-energy as emphasized by the solid line, which is a fit with Eq. (7) for $n=2,3$. The prefactors A_2 and A_3 contain all factors independent of x. The ratios $r_s=A_3/A_2$ of the fitted values of these prefactors are listed in Table I under ''Raman experiments.'' Note that two points, which are represented by dashed triangles, have not been included in the fit since they deviate unreasonably from the other data.

It is difficult to see with the naked eye in Fig. 3 the asymmetric behavior versus x, which may arise from third-order perturbation terms. The asymmetry appears, however, rather clearly when the difference between the measured (or the calculated) behavior and the VCA line is plotted, as shown in Fig. 4. In this figure, the solid line also represents the fit to all experimental data (except the dotted triangles), the dot-

TABLE I. Characterization of the asymmetry of the phonon self-energy with respect to $x=0.5$ through the ratio $r_s=A_{3,s}/A_{2,s}$ and the concentration $x_{\max,s}$ with $s=\Delta,\Gamma$. These quantities are displayed for each elemental crystal that is realized as a binary isotopic system $m_{1-x}M_x$, with separate rows for the corresponding real and imaginary part. The Raman data are compared with theoretical results that are derived from perturbation theory (PTh, this work), the coherent potential approximation (CPA), and *ab initio* calculations. The values of the self-energies (Δ_2,Γ_2) are for $x=0.5$.

	Raman experiments			PTh		CPA		*ab initio* [e]	
$m_{1-x}M_x$	Δ_2 (cm^{-1}) $-\Gamma_2$ (cm^{-1})	r_Δ r_Γ	$x_{\max,\Delta}$ $x_{\max,\Gamma}$	r_Δ r_Γ	$x_{\max,\Delta}$ $x_{\max,\Gamma}$	r_Δ r_Γ	$x_{\max,\Delta}$ $x_{\max,\Gamma}$	r_Δ r_Γ	$x_{\max,\Delta}$ $x_{\max,\Gamma}$
$^{12}C_{1-x}{}^{13}C_x$	≈ 6[a] ≈ 3[a]	0.31 0.61	0.57 0.62	0.33 0.88	0.58 0.66	0.35 0.66	0.58 0.63	0.22 0.53	0.55 0.61
$^{28}Si_{1-x}{}^{30}Si_x$	1.18[b] 0.03[b]	≈ 0 0.53	0.50 0.61	0.26 0.52	0.56 0.61	0.25 0.64	0.56 0.63		
$^{70}Ge_{1-x}{}^{76}Ge_x$	1.06[c] 0.03[c]			0.33 0.66	0.58 0.63			0.30 0.74	0.57 0.64
$^{112}Sn_{1-x}{}^{124}Sn_x$	1.8[d] 0.02[d]			0.67 ≈ 1	0.63 ≈ 0.67				
$^{116}Sn_{1-x}{}^{124}Sn_x$	0.7[d] 0.02[d]			0.41 0.82	0.59 0.65				

[a]Values taken as average from Refs. 5–10.
[b]Reference 11.
[c]Reference 14.
[d]Reference 15.
[e]References 12,13.

dashed line represents CPA calculations while the dotted line is a fit to the asterisks which indicate points obtained in the *ab initio* calculations.[12,13] All data in Fig. 4 show a similar asymmetric behavior, with a maximum of $\Delta_{\rm dis}(x)$ at $x\approx 0.6$. This figure allows us to conclude that the real part of the self-energy due to isotopic disorder is well understood for diamond, including the superposition of second-order and third-order perturbation terms.

Similar degree of understanding has been reached for $\Gamma_{\rm dis}(x)$ as shown in Fig. 5. The x position of the maxima of $\Delta_{\rm dis}$ and $\Gamma_{\rm dis}$ determined from the experimental data agree with those obtained by perturbation theory [Eq. (9)] and also with the CPA and *ab initio* calculations (see Table I). Note that the r_Δ and r_Γ values under ''PTh'' are obtained from the experimental values of Δ_2 for $x=0.5$. These values are not affected by the third-order terms, which vanish for $x=0.5$. Moreover, the small anharmonic self-energies do not significantly affect Δ_2 since the latter is determined by an integral over the whole (basically harmonic) DOS.

Concerning the other elemental semiconductors, detailed experimental results with sufficient values of x to reach quantitative conclusions of the type found for diamond, are only available for Si.[11] These data for Si are shown in Figs. 6 and 7 (filled circles) together with the results of CPA calculations (filled squares). The latter show for $\Delta_{\rm dis}(x)$ a clear asymmetry with a maximum at $x_{\max,\Delta}\approx 0.56$. The quality and the number of the experimental points are not sufficient to conclude that an asymmetry exists but they cannot exclude it either. The measured absolute values of $\Delta_{\rm dis}(x)$ almost (not quite) agree within error bars with the calculated ones.

The corresponding experimental values of $\Gamma_{\rm dis}(x)$ (see Fig. 7) are about a factor of 2 lower than the calculated ones, although both show the asymmetric behavior ($x_{\max,\Gamma}\approx 0.62$) predicted by Eq. (17b). The reason for the discrepancy between the calculated and measured $\Gamma_{\rm dis}$ is to be sought in the mechanism responsible for it in Si.[11] Within the harmonic approximation $\Gamma_{\rm dis}=0$ for Si, Ge, and α-Sn, because the Raman frequency is at the maximum of the spectrum and thus corresponds to zero density of one-phonon states. The rather small, but non-negligible, observed value of $\Gamma_{\rm dis}$ results from the DOS induced at the Γ point by the anharmonic interactions responsible for the linewidth of the isotopically pure crystals. Thus, the widths observed for Si, as well as for Ge and α-Sn, correspond to fourth-order (twice disorder and twice anharmonicity) and higher-order terms. Under these conditions, we have no guarantee that the terms included in an anharmonic CPA calculation suffice to describe the experimental data, and agreement within a factor of two between theory and the small experimental values of $\Gamma_{\rm dis}$ is to be regarded as satisfactory at this point. Using this argument too, similar values of $\Delta_{\rm dis}$ are to be expected for these elemental crystals.

Although isotopic-disorder-induced effects have not been studied so extensively in Ge and α-Sn, there are some experimental results available for $x=0.5$ (Refs. 14,15) that can be compared with perturbation calculations. The latter, once contrasted with the measurements for $x=0.5$, provide reliable predictions for future experiments. The corresponding

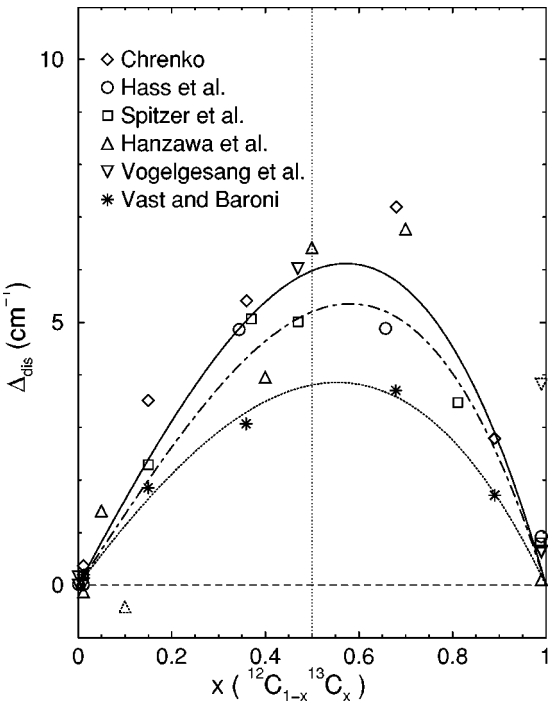

FIG. 4. Disorder-induced shift of the Raman phonon of diamond as a function of the ^{13}C concentration. The open symbols are Raman experimental data (Refs. 5–10) whereas the asterisks correspond to *ab initio* calculations (Refs. 12,13). The solid line is a fit with Eq. (7) for $n=2,3$ to all experimental data except for the two points at $x=0.1$ and $x=1$ indicated as dotted symbols. The dotted and dot-dashed lines represent the fits to theoretical values obtained from *ab initio* and CPA calculations, respectively.

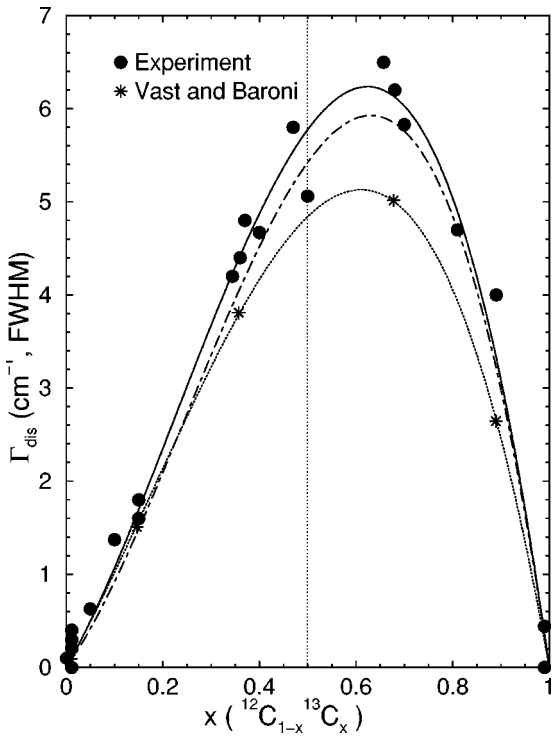

FIG. 5. Disorder-induced broadening of the Raman phonon of diamond as a function of the ^{13}C concentration. The filled circles have been obtained from the Raman data of Refs. 5–9 by taking into account the corresponding instrumental resolutions and subtracting the anharmonic broadening $\Gamma_{anh}\approx 2$ cm^{-1} (FWHM). The solid line is a fit with Eq. (7) for $n=2,3$ to these points. The dotted and dot-dashed lines are the corresponding fits to the values obtained from *ab initio* (Refs. 12,13) and CPA (Refs. 6,7) calculations, respectively. Note that the scatter of the experimental points around the fitted curve is considerably smaller than in Fig. 4. This is probably due to the fact that the widths measured for x around 0.5 are largely generated by the isotopic disorder while the disorder-induced shifts are a small addition to the VCA dependence on x (see Fig. 3).

data are displayed in Table I, where we compared them, in the case of Ge, with those obtained by *ab initio* calculations.[12,13] We should add that the *ab initio* values of Δ_{dis} for Ge calculated by Vast and Baroni[12,13] agree with the CPA calculation on Si and also represent the available experimental data rather well ($\Delta^{ab\ initio}(x=0.5)=1.14$ cm^{-1} compared to 1.18 and 1.06 cm^{-1} obtained experimentally for Δ_2 in Si and Ge, respectively). The *ab initio* calculations of Γ_{dis} for Ge, however, give values which are an order of magnitude larger than the experimental ones, a fact that can be attributed to numerical errors in the calculated DOS near the van Hove singularity which is found at the Raman frequency.

According to the values listed in Table I one can clearly distinguish between two different behaviors in the magnitudes of Δ_2 and Γ_2. Diamond exhibits a relatively large disorder-induced shift Δ_2, whereas the other elemental crystals have much smaller values. This largely reflects the factor of ω in Eq. (13b). The difference is even more striking for Γ_2, which nearly vanishes for Si, Ge, and α-Sn. This can be explained also by the different orders of perturbation theory coming into play. The overbending of the phonon dispersion of diamond introduces large (second-order) isotopic disorder effects which are not present in the case of Si, Ge, and α-Sn because of their vanishing DOS at the frequency of the Raman phonon. Such overbending of the phonon dispersion is also encountered in SiC and will be discussed in Sec. IV.

We also observe a slight but systematic upwards shift of $x_{\max,\Gamma}$ of the CPA values for Si, compared to those obtained by perturbation theory. The points of the CPA calculation, which includes higher-order perturbation terms, are fitted with Eq. (7) for $n=2,3$ that only contains the second-order and third-order terms. As shown in Fig. 1, the higher-order terms (such as, e.g., g_5) emphasize even more the asymmetric appearance of the self-energy, provided that the prefactors A_i are all positive. A fit with Eq. (7) for $n=2,3,4$ to the CPA values for the disorder-induced broadening of Si can be found in Ref. 11.

IV. EXTENSION FOR BINARY COMPOUNDS

The total isotopic-disorder-induced self-energy for a phonon of a binary compound[16] can be expressed as a sum of the self-energy contributions of the individual sublattices κ

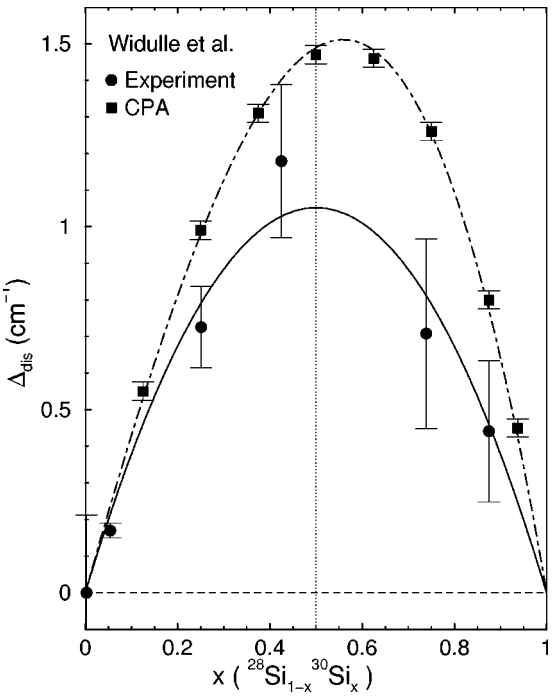

FIG. 6. Disorder-induced shift of the Raman phonon of Si as a function of the ^{30}Si concentration (Ref. 11). The solid line is a fit with Eq. (7) for $n=2,3$ to the experimental data. The dot-dashed line represents the corresponding fit to the values obtained from CPA calculations.

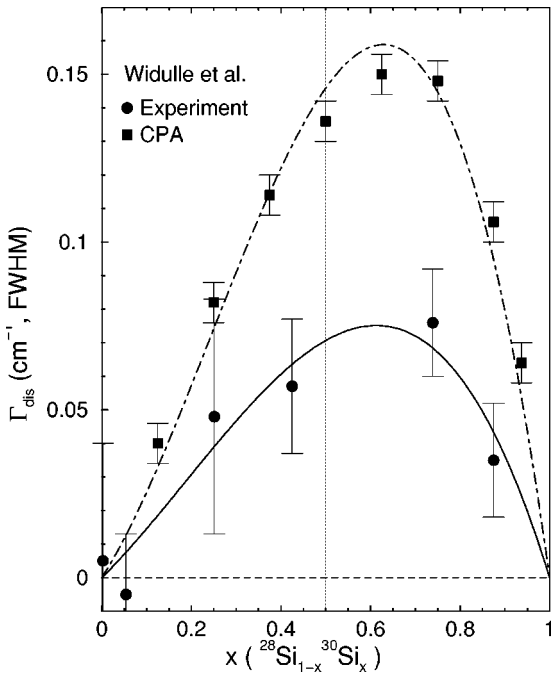

FIG. 7. Disorder-induced broadening of the Raman phonon of Si as a function of the ^{30}Si concentration (Ref. 11). The solid line is a fit with Eq. (7) for $n=2,3$ to the experimental data. The dot-dashed line represents the corresponding fit to the values obtained from CPA calculations.

$$\Pi_n(\omega,x)=\sum_\kappa \frac{g_n^\kappa(x)}{2^n}\omega|\mathbf{e}^\kappa(\omega)|^2 \times\left(\frac{1}{3N_c}\sum_i \omega_i D(\omega,\omega_i)|\mathbf{e}^\kappa(\omega_i)|^2\right)^{n-1}, \tag{21}$$

where $|\mathbf{e}^\kappa|^2$ denotes the square of the eigenvector, averaged over all $\mathbf{q}$'s corresponding to a given frequency. The second-order self-energy can be described in a way similar to that used for monoatomic semiconductors

$$\Delta_2(\omega,x)=\sum_\kappa \frac{g_2^\kappa(x)}{4}\omega|\mathbf{e}^\kappa(\omega)|^2 \times\left(\frac{1}{3N_c}\sum_i \omega_i|\mathbf{e}^\kappa(\omega_i)|^2\frac{\omega-\omega_i}{(\omega-\omega_i)^2+\gamma^2}\right), \tag{22a}$$

$$\Gamma_2(\omega,x)=\sum_\kappa \frac{g_2^\kappa(x)}{4}\omega|\mathbf{e}^\kappa(\omega)|^2 \times\left(\frac{1}{3N_c}\sum_i \omega_i|\mathbf{e}^\kappa(\omega_i)|^2\frac{\gamma}{(\omega-\omega_i)^2+\gamma^2}\right). \tag{22b}$$

For $\gamma\to 0$, Eq. (22b) simplifies to

$$-\Gamma_2(\omega,x)=\sum_\kappa \frac{g_2^\kappa(x)}{4}\omega|\mathbf{e}^\kappa(\omega)|^2 \times\left(\frac{1}{3N_c}\sum_i \omega_i|\mathbf{e}^\kappa(\omega_i)|^2\pi\delta(\omega-\omega_i)\right) =\sum_\kappa \frac{\pi}{12}g_2^\kappa(x)\omega^2|\mathbf{e}^\kappa(\omega)|^2\rho_1^\kappa(\omega), \tag{22c}$$

where $\rho_1^\kappa(\omega)$ corresponds to the one-phonon partial DOS projected on the sublattice κ. Note in Eq. (22c) that for crystals with diamond structure Eq. (13e) is recovered by setting $|\mathbf{e}^\kappa(\omega)|^2=1/2$.

The general expression for r_s can be quite complicated for binary compounds when both sublattices contain isotopic disorder. However, if there is only one isotopically disordered sublattice, the sum over κ is replaced by a single term. In this case, it is straightforward to derive expressions similar to Eqs. (17a) and (17b),

$$r_\Delta\simeq 8\frac{m}{\Delta m}\frac{1}{\omega|\mathbf{e}(\omega)|^2}\left[\frac{\Delta_2^2-\Gamma_2^2}{\Delta_2}\right]_{x=0.5}, \tag{23a}$$

$$r_\Gamma\simeq 16\frac{m}{\Delta m}\frac{1}{\omega|\mathbf{e}(\omega)|^2}[\Delta_2]_{x=0.5}, \tag{23b}$$

where $\mathbf{e}(\omega)$ is the eigenvector component at the disordered sublattice for the phonon under consideration (e.g., a Raman

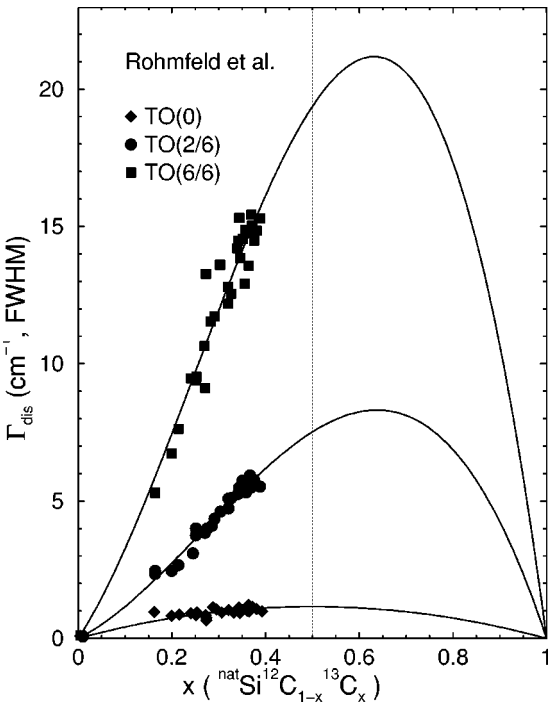

FIG. 8. Disorder-induced broadening of the TO Raman modes of the 6H-SiC polytype versus the ^{13}C concentration of the carbon sublattice. The data are taken from Ref. 17. The solid lines represent fits with Eq. (7) for $n=2,3$ to the data points that correspond to the TO(0), TO(2/6), and TO(6/6) phonon modes.

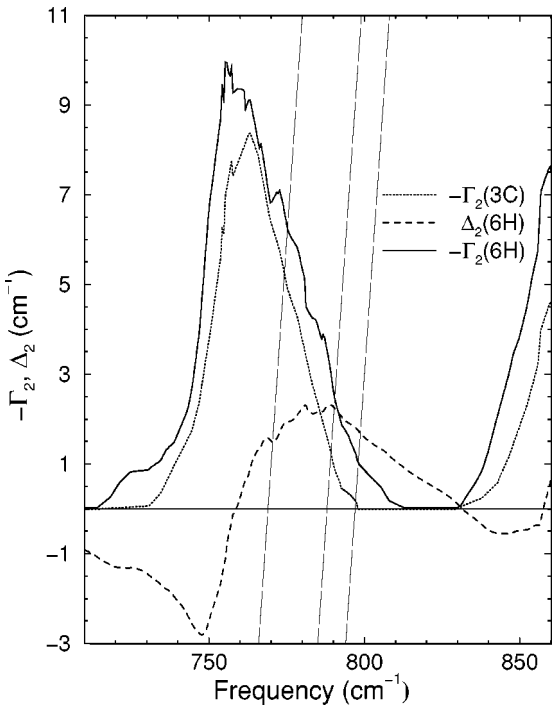

FIG. 9. Disorder-induced shift $\Delta_2(\omega)$ and broadening $\Gamma_2(\omega)$ for 3C-SiC and 6H-SiC. We obtain $\Gamma_2(\omega)$ from the DOS that has been calculated by Hofmann *et al.* (Ref. 19) using the bond-charge model. $\Delta_2(\omega)$ is determined by a Kramers-Kronig transformation.

phonon). Thus, the isotopic effects of a disordered sublattice in a compound is different from that for the corresponding monoatomic crystal.

We apply Eqs. (23a) and (23b) to the Raman spectroscopic results on a variety of $^{nat}Si^{12}C_{1-x}{}^{13}C_x$ polytypes, recently reported by Rohmfeld *et al.*[17] We have performed a fit with Eq. (7) for $n=2,3$ to the linewidth of the transverse optic (TO) modes of the 6H-SiC polytype measured in Ref. 17 for ^{13}C concentrations ranging from $x=0.15$ to $x=0.40$. These experimental results are displayed together with our fits in Fig. 8. The fit performed in Ref. 17 was based on the asymmetric curve obtained by CPA calculations for diamond.[7] This curve was first fitted to the data points of the TO(2/6) mode and further adjusted to the TO(0) and TO(6/6) modes by multiplication with the constant scaling factor $\omega^2\rho_1(\omega)$ assuming constant eigenvectors [see Eq. (22c)]. Instead, we have considered each TO mode separately and performed fits with Eq. (7) for $n=2,3$ in the same manner as for the elemental semiconductors in Sec. III. We used, however, parameters appropriate to SiC, not to diamond. In this way, we rigorously conclude that the behavior of Γ_{dis} versus x is asymmetric. This fact cannot be derived from the data in Fig. 3 of Ref. 17 which were obtained only for $0.15<x<0.40$. The latter can be fitted equally with either a symmetric or an asymmetric curve.

Using Eq. (22c) for a single disordered sublattice, together with the assumption of a constant eigenvector $|\mathbf{e}^{C}_{TO}(\mathbf{q})|=0.84$,[18–21] we have calculated the imaginary part $\Gamma_2(\omega)$ for 6H-SiC and 3C-SiC using the DOS of Hofmann *et al.*[19] The corresponding real part $\Delta_2(\omega)$ is obtained by the Kramers-Kronig relations. The frequency dependence of Δ_2 and Γ_2 for 6H-SiC, as well as Γ_2 for zinc blende SiC (3C-SiC) is shown in Fig. 9 for the region of the TO modes. The three parallel lines cut the x axis at the frequencies of the TO(0), TO(2/6), and TO(6/6) phonons, and the crossing with $\Delta_2(6H)$ gives the (approximate) disorder-induced shift of the corresponding Raman peak.

Raman experimental results extracted from Fig. 8 are compared in Table II with those found by the perturbation scheme of Eqs. (23a) and (23b). The fit to the TO(0) mode is symmetric, but the large scattering of data points still allows reasonable asymmetric fits with similar curvature than for the other two modes. The two numbers given for the ratio r_Δ of the TO(0) mode represent maximum and minimum values and correspond to 6H-SiC and 3C-SiC, respectively. For the cubic polytype the DOS vanishes at the Raman frequencies in the harmonic approximation. Therefore, we performed a convolution of the imaginary part with the anharmonic broadening $\Gamma_{anh}=1.4$ cm^{-1} (Ref. 22) in order to estimate the finite value. Note that the phonon dispersion of the hexagonal polytypes, calculated in Ref. 19, exhibits an overbending of the TO branches, which mainly occurs around the K point of the Brillouin zone. The relatively large value of Γ_2 observed for the TO(0) mode compared to those of Si, Ge, and α-Sn (see Table I) provides evidence of a nonvanishing DOS caused by an overbending of the phonon dispersion. The experimental results from Ref. 17 support therefore the DOS calculated with the bond charge model by Hofmann *et al.*[19].

The striking feature in Table II, which is added to the general behavior of the Raman phonons of elemental crys-

TABLE II. Asymmetry of the phonon self-energies of isotopically disordered SiC, characterized by the ratio $r_s = A_{3,s}/A_{2,s}$ and the concentration $x_{\max,s}$. Experimental results from Raman spectroscopy of the TO-phonons of 6H-SiC (Ref. 17) are compared with calculations using perturbation theory (PTh, this work). The values of the self-energies (Δ_2, Γ_2) are for $x = 0.5$.

	Raman experiment			PTh [a]		
$^{nat}Si^{12}C_{1-x}{}^{13}C_x$	Δ_2 (cm^{-1}) $-\Gamma_2$ (cm^{-1})	r_Δ r_Γ	$x_{\max,\Delta}$ $x_{\max,\Gamma}$	Δ_2 (cm^{-1}) $-\Gamma_2$ (cm^{-1})	r_Δ r_Γ	$x_{\max,\Delta}$ $x_{\max,\Gamma}$
				1.7	0.28–0.21	0.57
TO(0)	≈0.55	≈0	≈0.5	0.12–0.90	0.58	0.62
				2.2	−0.75	0.36
TO(2/6)	≈3.8	0.71	0.64	3.8	0.76	0.64
				1.5	−6.0	
TO(6/6)	≈9.7	0.66	0.63	7.3	0.53	0.61

[a]Note that for negative values the asymmetry is flipped with respect to $x = 0.5$, i.e. the maximum of the self-energy occurs at $x < 0.5$.

tals, is the negative values of r_Δ obtained for the TO(2/6) and TO(6/6) phonons. This change of sign implies a reversed asymmetry, i.e., the maximum is now shifted to lower concentrations of the heavier isotope ($x < 0.5$). Since in Ref. 17 the phonon frequency was used for the determination of the ^{13}C concentration, no experimental information can be extracted about the disorder-induced shift. Within our interpretation, however, a negative r_Δ has been already observed indirectly for a two-phonon combination in isotopically tailored diamond by cathodoluminescence.[23] The fact that some absolute values of $r_{\Delta,\Gamma}$ are much larger than unity is caused by a strong difference in magnitude between Δ_2 and Γ_2 or by a vanishing Δ_2 [see Eqs. (23a) and (23b)]. The latter occurs at frequencies near the maximum of the phonon DOS where $\Delta(\omega)$ changes sign.

V. CONCLUSIONS

General analytic expressions are given which allow the calculation of the real and imaginary parts of the self-energy of phonons due to isotopic disorder in elemental crystals (e.g., diamond-type semiconductors) to various orders of perturbation theory. The results are used to analyze the asymmetric behavior of these self-energies versus the isotopic concentration in crystals containing two different isotopes. The asymmetry is found to originate primarily from a combination of second-order and third-order contributions to the phonon self-energies and can be determined from the second-order perturbation terms without the need of additional parameters. These results are extended to binary crystals (e.g., zinc blende or wurtzite-type semiconductors) and used to interpret quantitatively recent experimental data for SiC versus the isotopic composition of the carbon component. The possible asymmetric behavior of the self-energy in this material, which contrary to the statement in Ref. 17 does not follow from the available data for $0.15 < x < 0.40$ only, is clarified on the basis of our analytical expressions.

ACKNOWLEDGMENTS

We would like to thank W. Kress for a careful reading of the manuscript. J. S. acknowledges support from the Max-Planck-Gesellschaft and the Ministerio de Educación y Cultura (Spain) through the Plan Nacional de Formación del Personal Investigador.

[1] G. D. Mahan, *Many-Particle Physics*, 2nd ed. (Plenum, New York, 1990), p. 94.
[2] S. I. Tamura, Phys. Rev. B **27**, 858 (1983).
[3] L. D. Landau and E. M. Lifschitz, *Course of Theoretical Physics*, 2nd ed. (Pergamon, Oxford, 1965), Vol. 3, p. 132.
[4] Note that $-\Gamma/2$ is positive whereas Δ can be either positive or negative.
[5] R. M. Chrenko, J. Appl. Phys. **63**, 5873 (1988).
[6] K. C. Hass, M. A. Tamor, T. R. Anthony, and W. F. Banholzer, Phys. Rev. B **44**, 12 046 (1991).
[7] K. C. Hass, M. A. Tamor, T. R. Anthony, and W. F. Banholzer, Phys. Rev. B **45**, 7171 (1992).
[8] J. Spitzer, P. Etchegoin, M. Cardona, T. R. Anthony, and W. F. Banholzer, Solid State Commun. **88**, 509 (1993); two points not included in this reference, measured for $x = 0.81$ and $x = 0.98$, have been added (see also Ref. 21).
[9] H. Hanzawa, N. Umemura, Y. Nisida, H. Kanda, M. Okada, and M. Kobayashi, Phys. Rev. B **54**, 3793 (1996).
[10] R. Vogelgesang, A. K. Ramdas, S. Rodriguez, M. Grimsditch, and T. R. Anthony, Phys. Rev. B **54**, 3989 (1996).
[11] F. Widulle, T. Ruf, M. Konuma, I. Silier, M. Cardona, W. Kriegseis, and V. I. Ozhogin, Solid State Commun. **118**, 1 (2001).
[12] N. Vast and S. Baroni, Phys. Rev. B **61**, 9387 (2000).
[13] N. Vast and S. Baroni, Comput. Mater. Sci. **17**, 395 (2000).
[14] J. M. Zhang, M. Giehler, A. Göbel, T. Ruf, and M. Cardona, Phys. Rev. B **57**, 1348 (1998).
[15] D. T. Wang, A. Göbel, J. Zegenhagen, and M. Cardona, Phys. Rev. B **56**, 13 167 (1997).

[16] S. I. Tamura, Phys. Rev. B **30**, 849 (1984).
[17] s. Rohmfeld, M. Hundhausen, L. Ley, N. Schulze, and G. Pensl, Phys. Rev. Lett. **86**, 826 (2001).
[18] For the TO modes of SiC, the variation of the eigenvectors $|e(\mathbf{q})|$ with $\mathbf{q}$ is small (Refs. 19,20,21).
[19] M. Hofmann, A. Zywietz, K. Karch, and F. Bechstedt, Phys. Rev. B **50**, 13 401 (1994).
[20] K. Karch, P. Pavone, W. Windl, O. Schütt, and D. Strauch, Phys. Rev. B **50**, 17 054 (1994).
[21] F. Widulle, T. Ruf, O. Buresch, A. Debernardi, and M. Cardona, Phys. Rev. Lett. **82**, 3089 (1999).
[22] C. Ulrich, A. Debernardi, E. Anastassakis, K. Syassen, and M. Cardona, Phys. Status Solidi B **211**, 293 (1999).
[23] T. Ruf, M. Cardona, H. Sternschulte, S. Wahl, K. Thonke, R. Sauer, P. Pavone, and T. R. Anthony, Solid State Commun. **105**, 311 (1998).